Physical Issues in Device Modeling: Length-Scale, Disorder, and Phase Interference

Nobuyuki Sano

Institute of Applied Physics

University of Tsukuba

Tsukuba, Ibaraki 305–8573

Email: sano.nobuyuki.gw@u.tsukuba.ac.jp

Abstract—The physical issues of device modeling associated with randomly doped impurities in nanoscale devices are discussed. We investigate the length-scale associated with the discrete impurities in the Drift-Diffusion simulation scheme and point out the importance of the self-consistency of the length-scales between the Poisson and transport equations. The physics behind the discrete impurity models is then discussed. The impurity-limited resistance of nanowires under various spatial configurations of impurities is also studied under the framework of the Lippmann-Schwinger theory. We show that there are two different and independent mechanisms leading to the variability in impurity-limited resistances; coherent and incoherent randomization processes. The physical origin of "self-averaging" under nanowire structures is then clarified.

I. Introduction

The complexity of the device structures as well as the shrinkage of the entire device dimension is being progressed to gain the benefit from the traditional scaling of nanoscale Si devices. As a result, there are still many physical issues in modeling ultra-scaled devices. Among others, the variability of device characteristics is now of crucial importance in integrating more than billions of nano-scale devices on a single chip. In the past 20 years or so, intensive studies on the variability have been carried out. Namely, the variability associated with randomly doped impurities, interface or line edge roughness, gate length deviation, grain boundaries of the gate materials, etc have been investigated [1].

In the present plenary talk, we would like to give a brief (and somewhat biased) overview of the physical issues of device modeling associated with randomly doped impurities in nanoscale devices.

We first discuss the length-scale associated with discrete impurities under the Drift-Diffusion (DD) simulation scheme [2]. Unfortunately, this issue has received very little attention so far. We point out the importance of the self-consistency of the length-scales between the Poisson and transport (current continuity) equations. Then, we discuss randomly doped impurities under nanostructures form the viewpoint of the impurity-limited resistance [3]. Namely, we discuss how the self-average in the impurity-limited resistance shows up under nanostructures. Notice that this is not simply a matter of statistics, but rather of phase interference among the impurities.

II. Length-Scale and Random Dopant Fluctuations

The physical origin of random dopant fluctuation (RDF) has been well known from the early stage of the investigations [2]; it is the modulation of the (long-range) electrostatic potential associated with the discreteness of doped impurities that leads to the fluctuations of the surface potential at the gate-oxide/substrate interface. In order to investigate the RDFs quantitatively, localized impurities, instead of continuous jelly impurities, are introduced in DD simulations. We would like to stress, however, that this jump from the traditional jelly model to a discrete model is not trivial at all. A naive introduction of a point charge into the Poisson equation to represent a localized impurity leads to a spiky potential, which causes an artificial carrier trap in the device substrate. In addition, this short-range potential is double-counted through the mobility model in the transport equations *unless the conventional mobility model is abandoned*. This implies that, depending on the transport equations employed in device simulations, some length-scale lies hidden behind the simulations.

A. Length-Scale in Poisson's Equation

The Poisson equation is usually considered to hold true at any length-scale. This is true in general. However, we should notice that the length-scale comes into play even in the Poisson equation by the way how the charge densities on the right-hand-side of Eq. (1) are described,

$$\nabla^2 \phi = -\frac{e}{\varepsilon_s} \left\{ p - n + N_d^+ - N_a^- \right\}. \tag{1}$$

Here, ϕ is the electrostatic potential, e the magnitude of elementary charge, ε_s the dielectric constant of the substrate, p the hole density, n the electron density, N_d^+ the ionized donor density, and N_a^- the ionized acceptor density.

As a concrete example, when impurities are represented by point charges, N_d^+ and N_a^- are expressed in terms of the Dirac delta-function. Then, there is no lower limit of the length-scale to describe the potential modulation. In other words, the potential modulation with any wavelength is included in Eq. (1). On the other hand, if the impurity density is represented by a scalar smooth function such as jelly impurity, the resolution of the potential modulation is limited by the mean-separation among the impurities. Hence, the potential modulation with

the wavelength shorter than the mean-separation is implicitly ignored from the simulations [4].

Since the carrier densities are determined by the transport equation, the length-scale imposed on the electrostatic potential is dependent of which transport equation is coupled with the Poisson equation. In other words, depending on the simulation schemes employed, the length-scale to be imposed on the Poisson equation becomes distinct.

B. Length-Scale in Drift-Diffusion Scheme

The DD equations consist of the current continuity equations for electrons and holes. They are derived from the first moment of the Boltzmann transport equation (BTE). The most significant approximation involved in their derivations is the local quasi-equilibrium approximation. This implies that the mean scattering time of inelastic scattering is so small that the system relaxes immediately to quasi-equilibrium with two independent quasi-Fermi potentials for electrons and holes. Therefore, the physical modulation with the wavelength shorter than the mean-free-path cannot be described, in principle, with the DD simulations.

Assuming that the mean scattering time is small enough, the localized impurities are screened by mobile carriers that leads to a *smoothly averaged* screened potential. The potential left behind the screening is the short-ranged scattering potential of impurity and ascribed to the reduction of mobility as impurity-limited resistance. This fact reflects in the impurity density dependence of the conventional mobility model incorporated into the DD simulations. Therefore, the short-range part of the Coulomb potential of impurity is already included in the conventional DD scheme. On the other hand, the long-range part of the impurity potential is compensated by the Coulomb potential of mobile carriers through screening and this physics is taken into account by solving the Poisson equation. Since the screening results from the long-range part of the Coulomb potential, it is the long-range-part of the impurity potential that should be included in the Poisson equation.

To summarize, it is mandatory to separate the Coulomb potential of ionized impurities into the short- and long-range parts. The separation is closely related to the screening process by the mobile carriers. Since the screening is dependent of the *average* carrier density in the device substrate, the cut-off parameter to extract the long-range part of the Coulomb potential becomes dependent of the carrier density in the device substrate. In other words, the cut-off parameter could be dependent of the gate voltage.

C. Discrete Impurity Models for Drift-Diffusion Simulation

In order to incorporate the long-range part of the Coulomb potential of impurities into the Poisson equation, we have proposed to cut off the short-range part of the potential by employing the finite-size charge distribution for each impurity [2]: The Fourier components beyond some critical value k_c of the charge density are discarded because they are already included as scattering potential in the mobility model. Then,

the charge distribution due to a single impurity located at the origin is spread in real space and expressed by

$$\rho_s^{long}(\mathbf{r}) = e\frac{k_c^3}{2\pi^2}\frac{\sin(k_c r) - (k_c r)\cos(k_c r)}{(k_c r)^3}, \qquad (2)$$

where k_c is roughly given by the inverse of the screening length, $k_c = 1/\lambda_{sc}$. The oscillatory behavior results from the sharp cut of the Fourier components. That is, the Fourier transform of $\rho_s^{long}(\mathbf{r})$ is simply given by

$$\rho_s^{long}(\mathbf{k}) = e\theta(k_c - k), \qquad (3)$$

where $\theta(x)$ is the Heaviside step function. The long-range part of the Coulomb potential is then given by

$$\phi_s^{long}(\mathbf{r}) = e\frac{k_c}{4\pi\varepsilon}\frac{2}{\pi}\frac{\mathrm{Si}(k_c r)}{k_c r} \qquad (4)$$

in MKS units. Here, $\mathrm{Si}(x)$ is the sine integral. Since $\mathrm{Si}(\infty) = \pi/2$, $\phi_s^{long}(\mathbf{r})$ approaches the ordinary bare Coulomb potential as $k_c r \to \infty$.

Another way to cut-off the short-range part of the Coulomb potential is to employ the Yukawa potential directly for the screened (short-range) Coulomb potential. The long-range part of the potential is then given by

$$\phi_Y^{long}(\mathbf{r}) = e\frac{k_c}{4\pi\varepsilon}\frac{1}{k_c r}\left(1 - e^{-k_c r}\right). \qquad (5)$$

As $k_c r \to \infty$, the potential $\phi_Y^{long}(\mathbf{r})$, of course, approaches the bare Coulomb potential. The corresponding charge distribution for a single impurity located at the origin is given by

$$\rho_Y^{long}(\mathbf{r}) = e\frac{k_c^3}{4\pi}\frac{e^{-k_c r}}{k_c r} \qquad (6)$$

and the Fourier transform of $\rho_Y^{long}(\mathbf{r})$ becomes

$$\rho_Y^{long}(\mathbf{k}) = e\frac{k_c^2}{k^2 + k_c^2}. \qquad (7)$$

Figure 1 shows the electrostatic potentials expressed by Eqs. (4) and (5). Although the potential profiles around the origin are different in the two models due to the different treatment of how the short-range components are discarded, both potentials coincide well at large distance and asymptotically approaches the bare Coulomb potential. The corresponding Fourier transforms of the charge density given by Eqs. (3) and (7) are also shown in the inset to Fig. 1. The components above k_c are sharply discarded in the first model, whereas the large components are gradually discarded in the second model. Notice that the zero-component of the Fourier transform of the charge density is included in both models and, thus, the total charge is conserved in both. The former dopant model is now widely employed in RDF simulations and simulation results could be found in the literature.

Nevertheless, we must admit that there are several problems in the above models. The above expressions of the finite-size impurity are valid only if the scattering potential is approximated with the Yukawa-like screened potential. This is correct as far as the device substrate is so large that we may
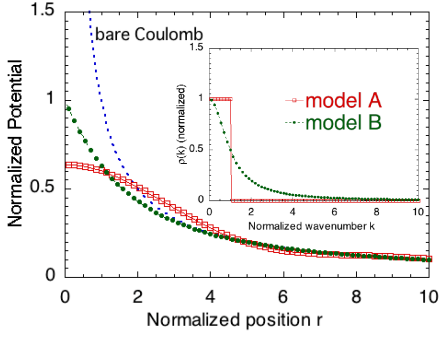
Fig. 1. Electrostatic potentials of a single impurity located at the origin obtained from the two different impurity models: Eqs. (4) (model A) and (5) (model B). The inset shows the corresponding Fourier transforms of the charge densities given by Eqs. (3) (model A) and (7) (model B).

ignore the effects associated with the boundaries such as the gate-oxide interface. In other words, the charge densities given by Eqs. (2) and (6) could be used only if impurities are doped in bulk structures. In addition, each impurity is treated as an independent scattering center in the mobility model. Hence, the scattering probability is proportional to the impurity density and the phase coherence among the impurities is ignored. If the correlation among multiple impurities is significant, the scattering strength is proportional to the multiple powers of impurity density, which leads to the Anderson localization at low temperature. In this sense, we might need to refine the conventional mobility model.

Those problems become serious as the device structure shrinks. That is, the modulation of the long-range potential could be strongly affected by the boundaries and each scattering center might be coherently coupled. The former problem is now under investigation and the latter is the issue to be discussed in the next section.

III. PHASE INTERFERENCE AND SELF-AVERAGING

The variability observed in mobility and/or resistance of nanowires has been studied via large-scale numerical simulations [5-6]. The phase interference among the impurities distributed randomly in the substrate is of crucial importance in understanding the physics behind such variability. In fact, the phase interference plays a dominant role in self-averaging the transport properties such as resistances in *long channel* devices [7]. Many different configurations of impurities in the substrate allows us to use the space-average impurity scattering rates in calculating the mobility etc, although the precise impurity configuration is different for each device.

A. Theoretical Backgrounbd

We consider a cylindrical nanowire with the radius of $r_s = 2$ nm and the impurity density in the substrate is assumed to be uniform ($n_{imp} = 2 \times 10^{19}$ cm^{-3}). The channel length L of the wire changes in accordance with the number of impurities doped in the channel region. In addition, the extreme quantum limit, in which only the lowest subband is involved in electron

transport, is assumed in which the effects of phase interference is most significant.

The conductance G of nanowires is calculated from the Landauer formula under the linear response regime. It should be noted, however, that the total resistance R_{tot} ($= 1/G$) is comprised of two contributions; the contact resistance and the channel resistance [3]. The former results from the difference in the number of modes between the lead and the reservoirs, whereas the latter is due to *both* the short-range potential modulations by scatterers *and* the long-range potential modulation. This long-range potential modulation also consists of the long-range part of the Coulomb potential of charged particles (impurities and carriers) and the electrostatic potential induced by the applied gate voltage. In general, this long-range potential modulation is irrelevant to the channel resistance and simply ascribed to the carrier density modulation in the channel. As the channel length shrinks, direct tunneling from the source to the channel and/or the drain regions comes into play and finite resistance shows up.

In order to extract the impurity-limited resistance from the total resistance, we intentionally eliminate phonon scattering and consider only impurity scattering. Furthermore, the resistance caused by the long-range potential modulation mentioned above is ignored by assuming that the channel potential is flat along the wire axis. As a consequence, the impurity-limited resistance is obtained simply by subtracting the contact (quantum) resistance from the total resistance, $R_s = R_{tot} - R_0$ with $R_0 = \pi\hbar/e^2$. The transmission and the reflection coefficients are calculated from the asymptotic form of the scattered wave function by solving the Lippmann-Schwinger (LS) equation. By assuming the short-range δ-function potential for localized impurities, the exact transmission and reflection coefficients could be derived.

B. Variability and Phase Interference

The calculation results show that the impurity-limited resistance R_s scatters over a few orders of magnitudes. Such large fluctuations result from two different physical origins: The fluctuations in R_s in the transverse direction (impurities are fixed at the same position on the wire axis) are attributed to the variations in the subband wavefunctions, whereas the fluctuations along the longitudinal (wire axis) direction are due to the phase interference of electrons among the impurities. Therefore, the former has nothing to do with the phase correlation among multiple impurities; each impurity could be regarded as independent. Since the central-limit theorem could be applied in this case, the fluctuations with respect to the transverse direction diminish as the channel length becomes longer. On the other hand, the variations in R_s along the axis direction do not generally vanish even for long channel wires, as noted by Kohn and Luttinger [7].

In order to demonstrate this point, we eliminate the fluctuations associated with the subband wavefunctions; we carry out similar calculations by placing several impurities *on the wire axis* at temperature $T = 300$ K. The calculation results for the cases of three or four (acceptor or donor) impurities
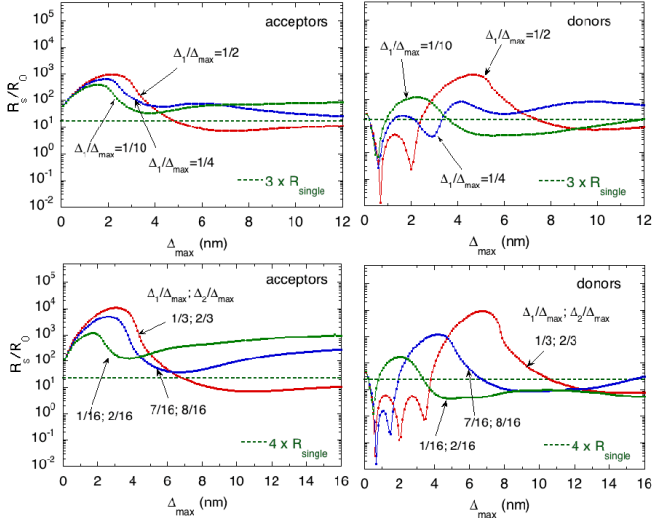
3

Fig. 2. Impurity-limited resistances of three (top) and four (bottom) acceptor or donor impurities at $T = 300$ K as a function of the maximum separation of impurities Δ_{max}. All impurities are located on the wire axis. The horizontal dotted lines show the uncorrelated values, $3R_{single}$ and $4R_{single}$, with R_{single} being the single-impurity resistance located on the wire axis.

are shown in Fig. 2 as a function of the maximum separation among the impurities Δ_{max}. The uncorrelated (classical) values of the resistatace are also indicated with the horizontal dotted lines. A large oscillatory behavior in R_s is observed in the first few nm, which results from the constructive or dstructive phase interference among the impurities. On the other hand, R_s nearly stays constant as Δ_{max} becomes large. This is somewhat surprising because no averaging over the configuration of impurities nor energy dissipating scattering which randomizes electron's phase is included in the above analyses. In other word, the phase randomization is taking place *even under the fully coherent circumstances under each specific impurity configuration.*

C. Physical Origin of Self-Averaging

We find that the physical origin of this phase randomization along the wire axis direction is closely related to the broadness of the energy spectrum of in-coming electrons from the reservoirs (source and drain). That is, R_s is averaged by in-coming electrons with many different kinetic energies when the spectrum is broad (temperature of *the reservoirs* is high). This phase randomization is, therefore, partially responsible to the self-averaging. If temperature is low enough such that the energy spectrum of the in-coming electrons is limited to be a very narrow range around the Fermi energy of the reservoirs, the phase coherence lasts longer distances and R_s deviates from the uncorrelated value even at large Δ_{max}.

However, as is clear from Fig. 2, the values of R_s at large Δ_{max} scatter to some extent around the uncorrelated values. This results from the fact that the transmission probability T_A is very close to zero at such large impurity separation ($\Delta_{max} \geq 10$ nm) and electrons hardly go through the channel

region. As a result, R_s is greatly affected by a tiny fluctuation in T_A and scatter around the uncorrelated value, $3R_{single}$ or $4R_{single}$. We should notice, however, that at room temperature, phonon scattering is always inevitable even in nanoscale channels [8]. Since its mean-free-path is around 10 nm, the phase coherence is almost always destroyed at such large impurity separation. Then, the ensemble-average over various impurity configurations again comes into play in long channel nanowires. In other words, the phase coherence is destroyed at large Δ_{max} and the variations even along the axis direction vanish due to incoherent averaging over various impurity configurations, in addition to the phase randomization.

IV. CONCLUSIONS

The length-scale associated with RDFs in the DD simulations has been discussed. We have pointed out the importance of the self-consistency in length-scale between the Poisson and transport equations. We have also investigated the variability in the impurity-limited resistances due to localized impurities in nanowires. The self-averaging is mainly ascribed to the broadness of the energy spectrum of in-coming electrons from the reservoirs, in addition to phase breaking scattering.

REFERENCES

[1] A. Asenov, A. R. Brown, J. H. Davies, S. Kaya, and G. Slavcheva, "Simulation of intrinsic parameter fluctuations in decananometer and nanometer-scale mosfets," *IEEE Trans. Electron Dev.*, vol. 50, no. 9, pp. 1837–1852, 2003.
[2] N. Sano, K. Matsuzawa, M. Mukai, and N. Nakayama, "Role of long-range and short-range coulomb potentials in threshold characteristics under discrete dopants in sub-0.1 μm Si-MOSFETs," in *Technical Digest. Int. Electron Device Meeting, 2000*, pp. 275–278.
[3] N. Sano, "Impurity-limited resistance and phase interference of localized impurities under quasi-one dimensional nano-structures," *J. Appl. Phys.*, vol. 118, no. 24, 2015.
[4] N. Sano, K. Matsuzawa, M. Mukai, and N. Nakayama, "On discrete random dopant modeling in drift-diffusion simulations: physical meaning of 'atomistic' dopants," *Microelectronics Reliability*, vol. 42, no. 2, pp. 189 – 199, 2002.
[5] M. P. Persson, H. Mera, Y.-M. Niquet, C. Delerue, and M. Diarra, "Charged impurity scattering and mobility in gated silicon nanowires," *Phys. Rev. B*, vol. 82, p. 115318, Sep 2010.
[6] A. Martinez, M. Aldegunde, N. Seoane, A. Brown, J. Barker, and A. Asenov, "Quantum-transport study on the impact of channel length and cross sections on variability induced by random discrete dopants in narrow gate-all-around silicon nanowire transistors," *IEEE Trans. Electron Dev.*, vol. 58, no. 8, pp. 2209–2217, Aug 2011.
[7] W. Kohn and J. M. Luttinger, "Quantum theory of electrical transport phenomena," *Phys. Rev.*, vol. 108, pp. 590–611, Nov 1957.
[8] N. Sano, "Kinetics of quasiballistic transport in nanoscale semiconductor structures: Is the ballistic limit attainable at room temperature?" *Phys. Rev. Lett.*, vol. 93, p. 246803, Dec 2004.